SUPPLEMENT

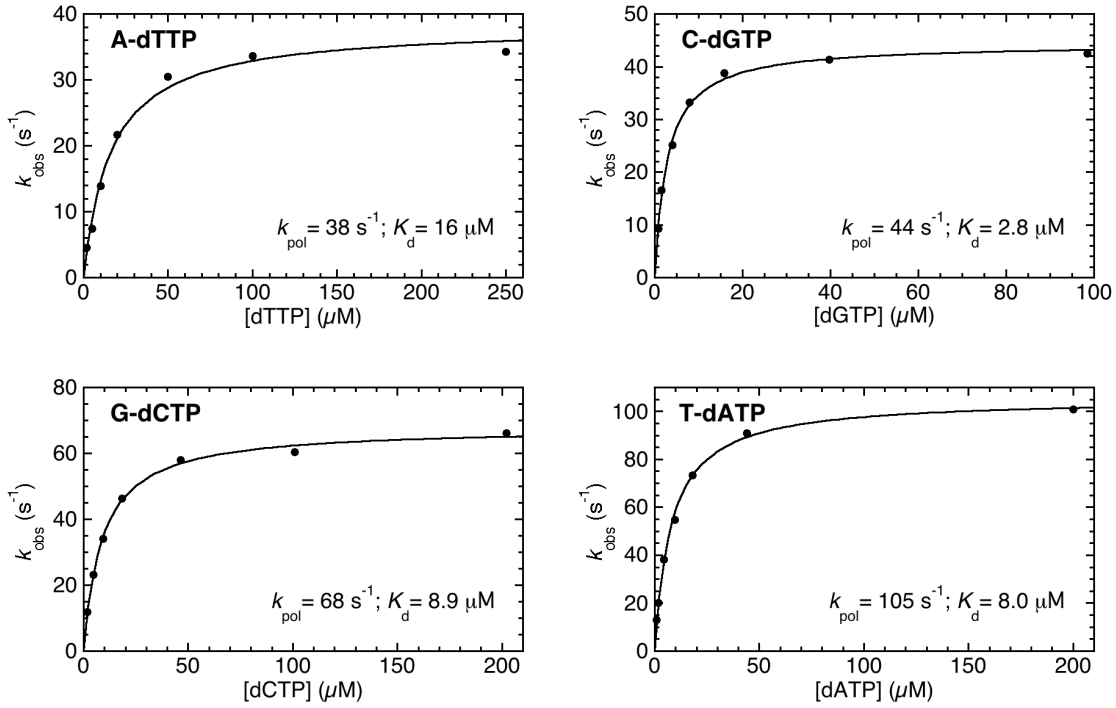

Figure S1. Kinetics of complementary nucleotide incorporation by WT Pol I(KF) at all 4 template bases. Single-turnover rates were measured as described in Experimental Procedures, using the DNA substrates shown in Figure 2A. These results, plus a duplicate set of measurements, provided the data in Table 1.

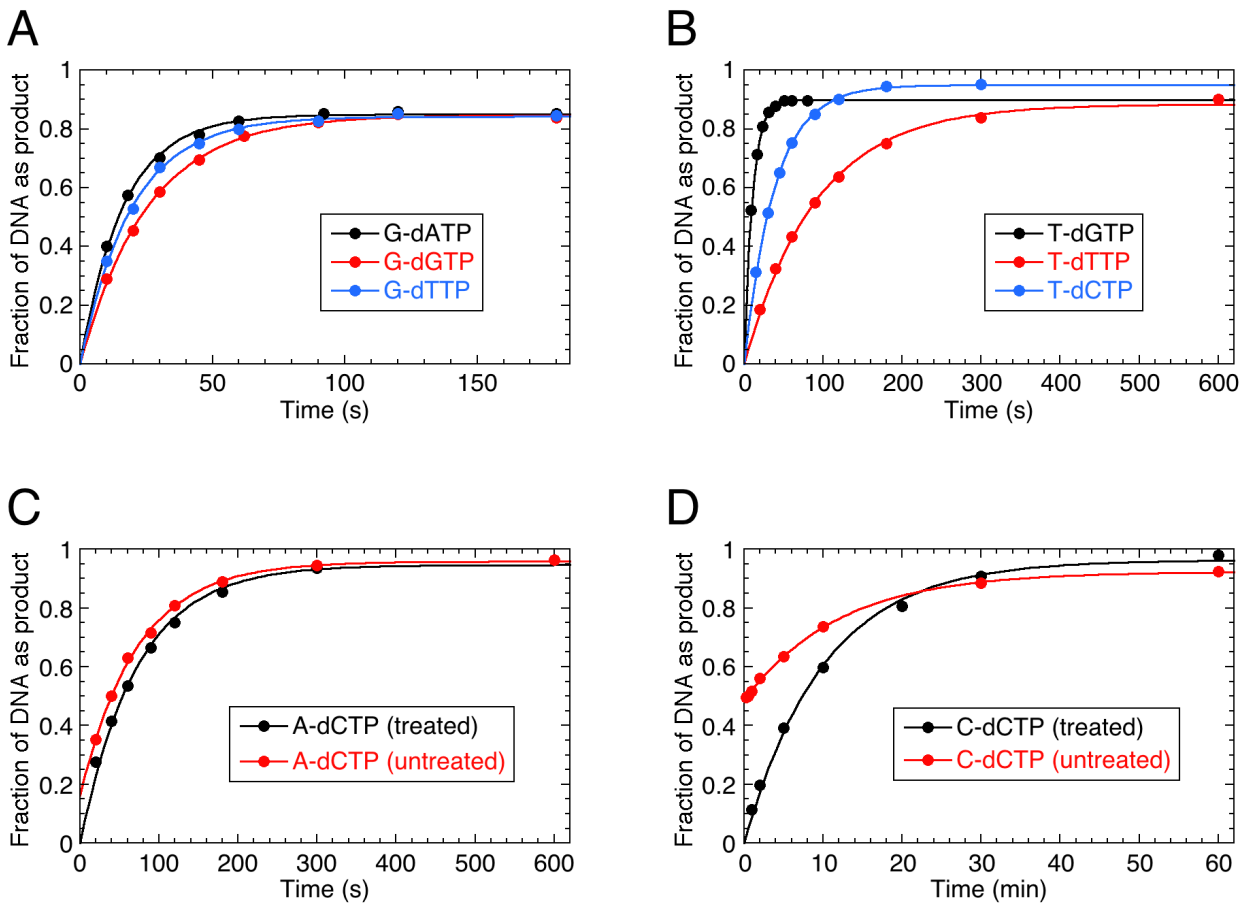

Figure S2. Misinsertion reactions catalyzed by WT Pol I(KF). A. Example of reaction time courses for all three misinsertion reactions at template G. B. Example of reaction time courses at template T. Panels C and D show the effect of pretreating dNTPs to remove miscoding contaminants, exemplified by dCTP (panel C), which is usually contaminated with dUTP, and by another batch of dCTP (panel D) which contained an unknown contaminant whose coding behavior resembled dGTP.

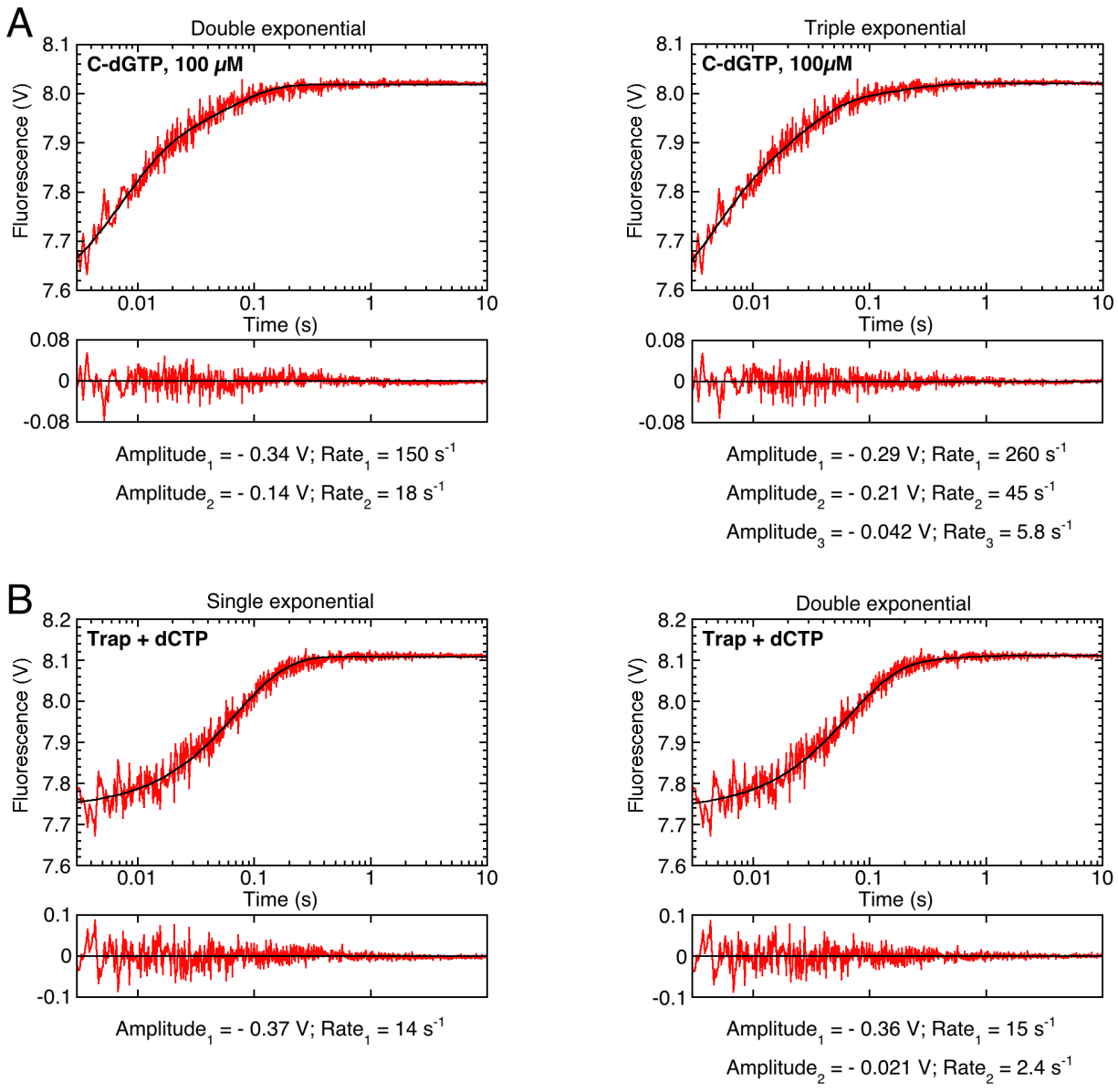

Figure S3. Examples of curve fitting and residuals for stopped-flow fluorescence data. A. The 100 μM dGTP trace from Figure 3A was fitted to double or triple exponentials, giving the parameters listed under each plot. In this example, the triple exponential improved the fit. B. The dCTP trace from the FRET assay of DNA dissociation in Figure 11A. When the data were fitted to single or double exponentials; there was very little improvement in the fit using the double exponential, indicating that a single exponential is sufficient to describe this fluorescence change.

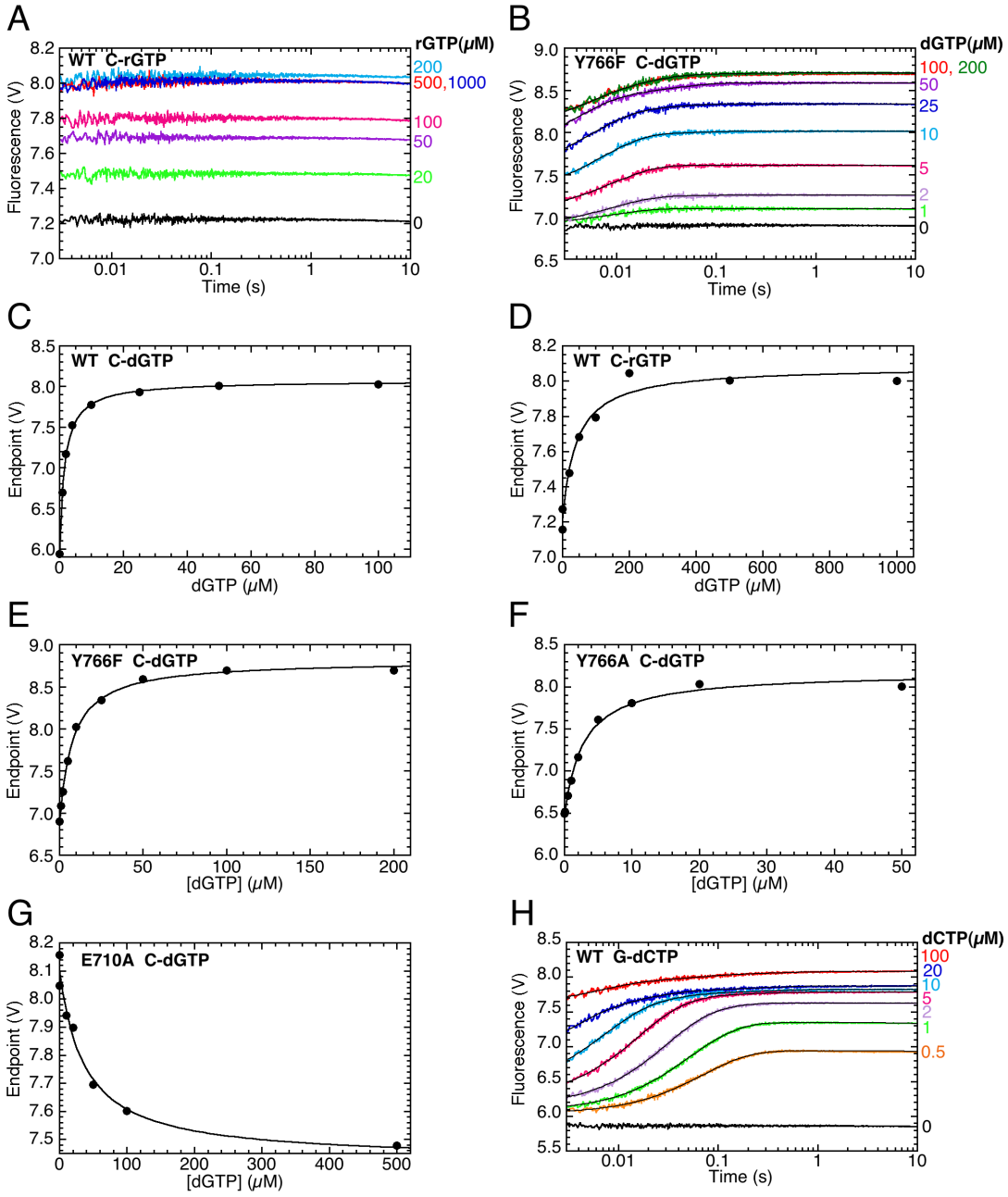

Figure S4. Determination of $K_{d\ overall}$ for nucleotide binding from stopped-flow data using the T(+1)2-AP probe. A. Fluorescence traces obtained with WT Pol I(KF) on addition of rGTP, at the indicated concentrations, opposite a template C. B. A similar experiment observing dGTP addition opposite a template C by Y766F. Plots of the endpoints of the fluorescence traces *vs.* nucleotide concentration for these experiments are shown in panels D and E, respectively. Panels C, F and G show the plots corresponding to the experiments in Figure 3. In panels C to G, $K_{d\ overall}$ was obtained by fitting the data to a hyperbolic equation. H. Titration of dCTP addition opposite template G by WT Pol I(KF).

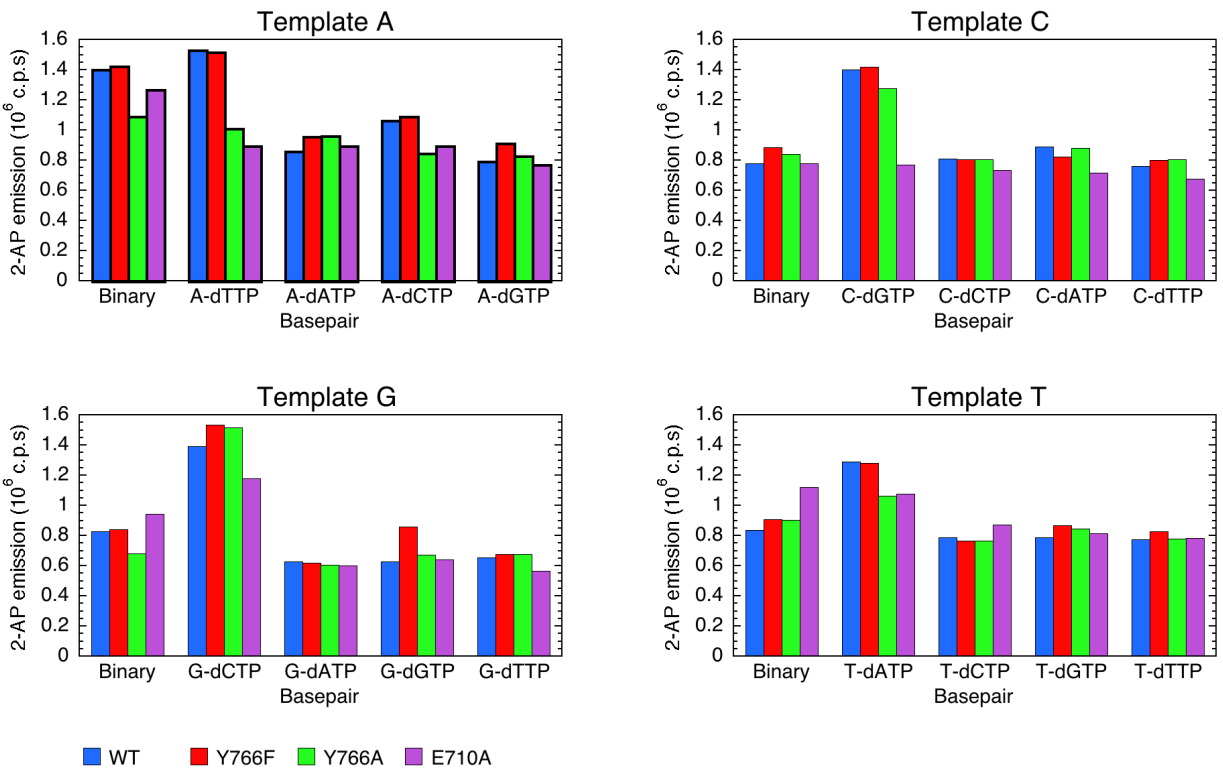

Figure S5. Fluorescence emission spectra of T(+1)2-AP DNAs with all 4 template bases (Figure 2B), as binary complexes and ternary complexes with complementary and mispaired dNTPs. The bars indicate the fluorescence signal at the 2-AP emission maximum after appropriate corrections (see Experimental Procedures). For each group of four bars, the same DNA-dNTP mix was scanned at the identical instrument settings with each of the proteins, confirming many of the differences that we suspected from the stopped-flow data, e.g. that the 2-AP signal from the G-dGTP basepair is unusually high with Y766F.

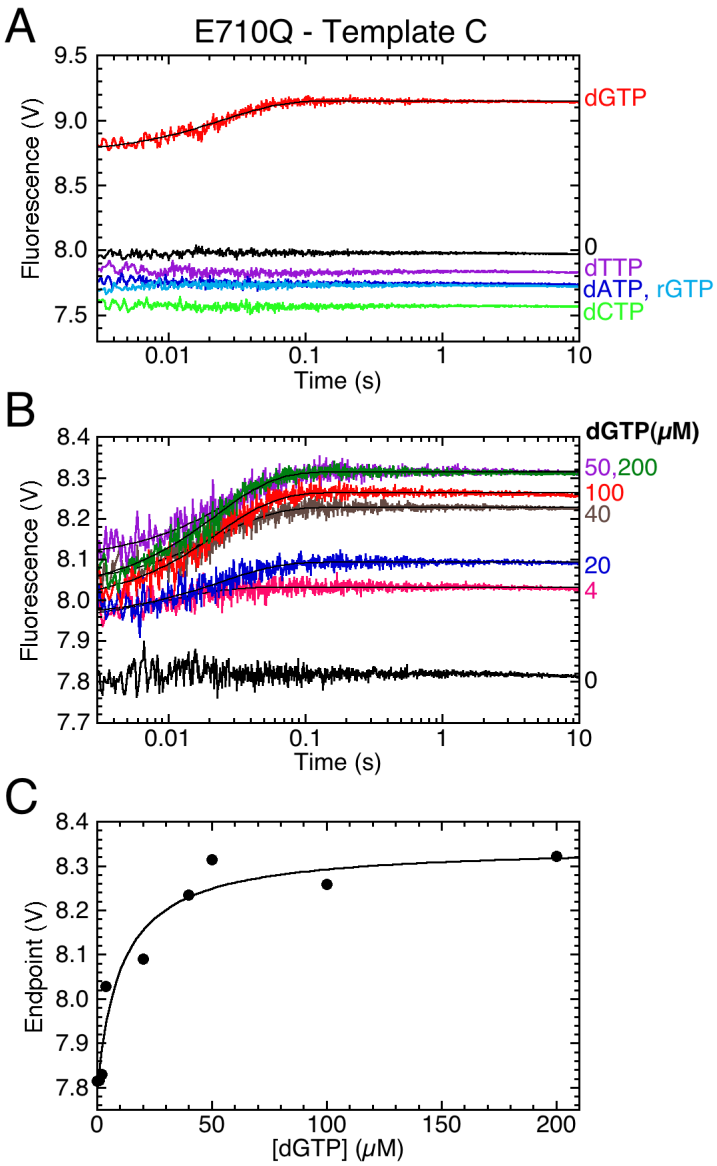

Figure S6. Stopped-flow fluorescence experiments with E710Q Pol I(KF) using the T(+1)2-AP DNA duplex with a template C (Figure 2B). A. Fluorescence traces obtained on addition of correct or mismatched dNTPs (1 mM final concentration) to a binary complex. The trace marked "0" corresponds to the addition of reaction buffer, showing the fluorescence of the binary complex. B. Titration experiment showing the changes in 2-AP fluorescence on addition of dGTP, at the indicated concentrations, to the binary complex. In A and B, the black lines superimposed on some of the data traces show fitting to single exponential equations, giving the parameters reported in Table S1. C. Determination of $K_{\text{d overall}}$ for dGTP binding by plotting the endpoints of the fluorescence traces in B *vs.* nucleotide concentration and fitting the data to a hyperbolic equation.

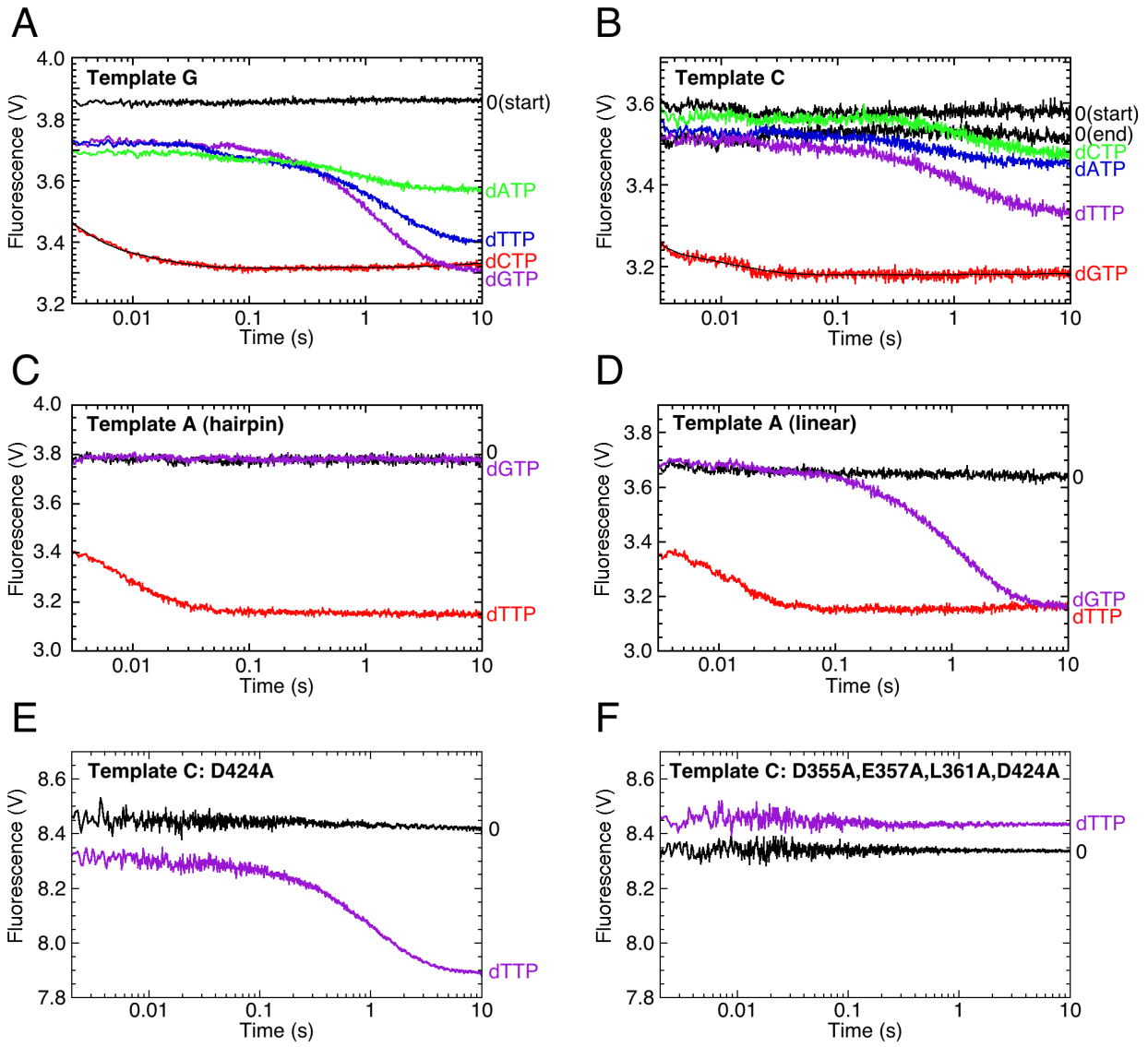

Figure S7. Stopped-flow fluorescence data using 744-AEDANS Pol I(KF) and T(-8)dabcyl DNA substrates to report the fingers-closing conformational change. A and B. The DNA substrates were linear dabcyl-containing duplexes (Figure 2D). Complementary dNTPs were present in the reaction at 50 μM, and mispaired nucleotides at 1 mM. The complementary dNTP traces were fitted to double exponential equations (black lines), giving the parameters reported in Table S2. C. The DNA substrate was a hairpin dabcyl-containing duplex with A as the templating base (Figure 2E). The complementary dTTP was present in the reaction at 50 μM, and the mispaired dGTP at 1 mM. D. As C, except that a linear DNA with template A (Figure 2D) was used. E. Binding of mispaired dTTP (at 1 mM final concentration) to the binary complex of our standard "WT" Pol I(KF) (having the D424A mutation at the 3'-5' exonuclease site) with a linear dabcyl-containing duplex DNA with a template C (Figure 2D). F. As E, except that the Pol I(KF) had 4 mutations at the exonuclease site (D355A,E357A,L361A,D424A), diminishing DNA binding affinity at this site (*17*).

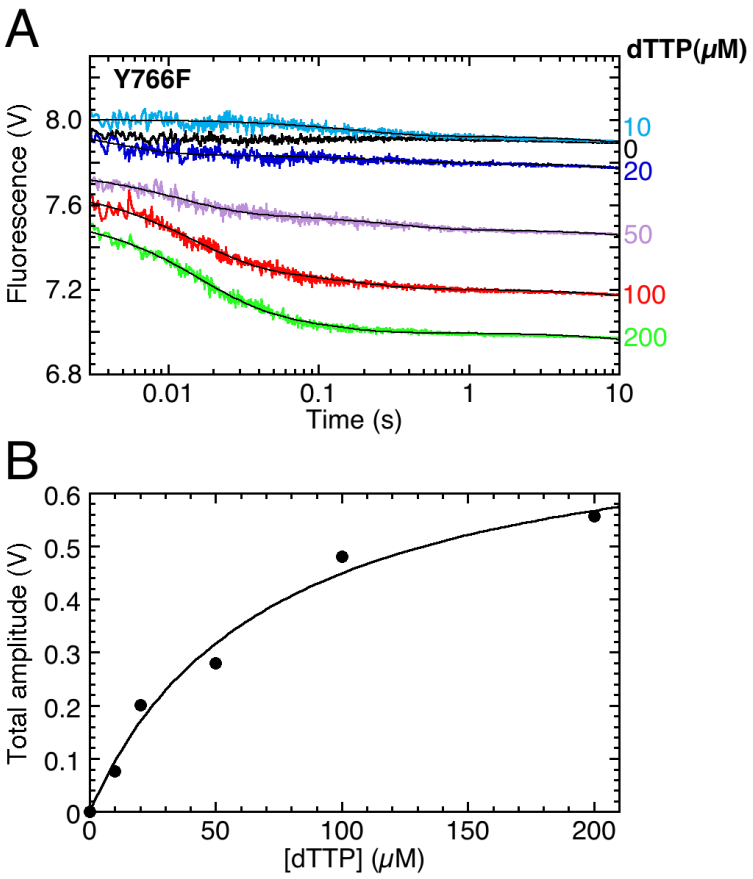

Figure S8. Nucleotide concentration dependence of the fingers-closing step for Y766F, using the FRET-based AEDANS-Dabcyl assay. A. Titration experiment showing the fluorescence changes observed on addition of dTTP, at the indicated concentrations, to a binary complex of Y766F with the template-A hairpin dabcyl DNA (Figure 2E). The black lines superimposed on the data traces show fitting to double exponential equations, giving the parameters reported in Table S2. B. Determination of $K_{\text{d overall}}$ for dTTP binding by plotting the endpoints of the fluorescence traces in A *vs.* nucleotide concentration and fitting the data to a hyperbolic equation.

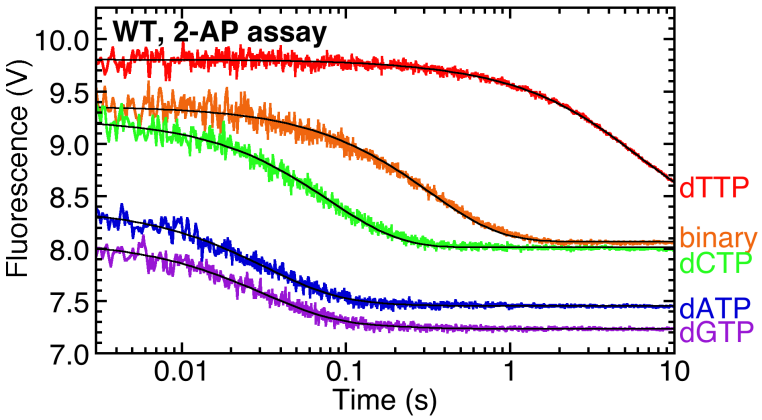

Nucleotide	k_{off} (s^{-1}) (FRET)	k_{off} (s^{-1}) (2-AP)
none	3.1 ± 0.2	2.7 ± 0.5
dTTP	0.80 ± 0.07	0.18
dATP	29 ± 0.4	31 ± 4
dCTP	14 ± 0.14	17 ± 6
dGTP	26 ± 3	32 ± 6
rUTP	19 ± 0.3	

Figure S9. DNA dissociation from WT Pol I(KF) measured by stopped-flow fluorescence using the T(+1)2-AP reporter with A as the templating base (Figure 2B). The 2-AP fluorescence decreases when the DNA duplex is released from Pol I(KF) and prevented from rebinding by an excess of an unmodified DNA duplex, serving as a trap. The orange trace is the dissociation of the Pol-DNA binary complex without additional dNTPs. The other traces show the dissociation of the ternary complex, measured by including 2 mM of a complementary (dTTP) or noncomplementary deoxynucleotide in the DNA trap solution. The black lines superimposed on the traces show fitting to single or double exponential equations; the dissociation rates (see Table) agree well with those measured using the FRET-based assay in Figure 11A.

Table S1: Curve-fitting parameters derived from stopped-flow experiments with a 2-AP reporter, reported in Table 3.[a]

WT: C-dGTP titration (Fig. 3A)						
dGTP(μM)	**A_1(V)**	**k_1(s^{-1})**	**A_2(V)**	**k_2(s^{-1})**	**A_3(V)**	**k_3(s^{-1})**
1	-0.58	85	-0.13	39		
2	-0.96	87	-0.048	16		
4	-1.1	140	-0.13	25		
10	-0.96	190	-0.096	20		
25	-0.55	880	-0.44	160	-0.12	18
50	-0.41	190	-0.13	28	-0.030	3.6
100	**-0.29**	**260**	**-0.21**	**45**	**-0.042**	**5.8**
Y766F: C-dGTP titration (Fig. S3B)						
dCTP(μM)	**A_1(V)**	**k_1(s^{-1})**	**A_2(V)**	**k_2(s^{-1})**	**A_3(V)**	**k_3(s^{-1})**
1	-0.21	110				
2	-0.38	110	-0.019	14		
5	-0.58	110				
10	-0.75	140	-0.044	17		
25	-0.73	190	-0.12	34		
50	-0.70	260	-0.19	30		
100	-0.47	180	-0.16	50	-0.030	6.3
200	-0.42	250	-0.29	59	-0.021	3.4
Y766A: C-dGTP titration (Fig. 3B)						
dGTP(μM)	**A_1(V)**	**k_1(s^{-1})**	**A_2(V)**	**k_2(s^{-1})**	**A_3(V)**	**k_3(s^{-1})**
0.5	-0.24	70				
1	-0.39	76				
2	-0.62	89				
5	-0.90	110				
10	-0.97	180	-0.14	46		
20	-0.93	160	-0.047	12		
50	-0.88	190	-0.096	28		
E710A: C-dGTP titration (Fig. 3C)[b]						
dGTP(μM)	**A_1(V)**	**k_1(s^{-1})**	**A_2(V)**	**k_2(s^{-1})**	**A_3(V)**	**k_3(s^{-1})**
100	0.82	730	-0.043	38		
500	0.65	620	-0.10	68		
E710Q: C-dGTP titration (Fig. S6B)						
dGTP(μM)	**A_1(V)**	**k_1(s^{-1})**	**A_2(V)**	**k_2(s^{-1})**	**A_3(V)**	**k_3(s^{-1})**
4	-0.082	94				
20	-0.13	42				
40	-0.19	44				
50	-0.22	36				
100	-0.27	44				
200	-0.29	45				

WT						
Reaction (μM dNTP)	**A_1(V)**	**k_1(s^{-1})**	**A_2(V)**	**k_2(s^{-1})**	**A_3(V)**	**k_3(s^{-1})**
A-dTTP(1000) Fig. 4	**-0.84**	**95**	**-0.13**	**25**	**-0.039**	**3.2**
A-dTTP(1000) expt 2	**-0.99**	**100**	**-0.11**	**20**	**-0.047**	**3.7**
A-dTTP(1000) expt 3	**-0.92**	**86**	**-0.12**	**19**	**-0.051**	**3.8**
C-dGTP(1000) Figs. 4,6A	**-0.37**	**120**	**-0.14**	**34**	**-0.041**	**3.8**
C-rGTP(1000) Fig. 6A	**-0.19**	**94**				
G-dCTP(1) Fig. 4	-0.54	36	-0.83	16		
T-dATP(1000) Fig. 4	**-0.41**	**410**	**-0.084**	**43**	**-0.035**	**2.0**
T-dATP(1000) expt 2	**-0.31**	**350**	**-0.078**	**33**	**-0.037**	**2.3**
T-dATP(100) Fig. 4	**-0.25**	**230**	**-0.062**	**27**	**-0.037**	**2.1**
2-AP-dTTP (100) Fig. 7	0.584	520	0.15	115		
2-AP-dTTP (500) Fig. 7	0.238	339	0.106	64		
Y766F						
Reaction (μM dNTP)	**A_1(V)**	**k_1(s^{-1})**	**A_2(V)**	**k_2(s^{-1})**	**A_3(V)**	**k_3(s^{-1})**
A-dTTP(1000) Fig. 4	**-0.56**	**72**	**-0.060**	**6.7**		
A-dTTP(1000) expt 2	**-0.57**	**76**	**-0.054**	**7.8**		
C-dGTP(10) Fig. 4	-0.72	170	-0.070	16		
C-dGTP(1000) Fig. 6B	**-0.53**	**110**	**-0.064**	**12**		
C-dGTP(1000) expt 2	**-0.52**	**110**	**-0.053**	**9.8**		
G-dCTP(1)*	**-0.49**	**68**				
T-dATP(10)*	-0.83	130	-0.033	12		
Y766A						
Reaction (μM dNTP)	**A_1(V)**	**k_1(s^{-1})**	**A_2(V)**	**k_2(s^{-1})**	**A_3(V)**	**k_3(s^{-1})**
A-dTTP(1000) Fig. 4	**-0.45**	**110**	**0.041**	**4.9**		
A-dTTP(1000, expt 2)	**-0.21**	**150**	**0.047**	**6.6**		
A-dTTP(1000, expt 3)	**-0.32**	**100**	**0.036**	**5.9**		
A-dTTP(1000, expt 4)	**-0.28**	**100**	**0.073**	**5.1**		
A-dTTP(1000, expt 5)	**-0.31**	**110**	**0.056**	**2.1**		
A-dTTP(1000, expt 6)	**-0.31**	**140**	**0.064**	**4.6**		
C-dGTP(10) Fig. 4	-1.2	140	-0.077	7.8		
C-dGTP(1000) Fig. 6C	**-0.67**	**180**	**-0.10**	**38**		
C-dGTP(1000) expt 2	**-1.0**	**140**	**-0.050**	**19**		
C-dGTP(1000) expt 3	**-0.71**	**180**	**-0.066**	**25**		
C-rGTP(1000) Fig. 6C	**-0.56**	**170**	**-0.0086**	**97**		
C-rGTP(1000, expt 2)	**-0.52**	**200**	**-0.048**	**49**		
G-dCTP(10) Fig. 4	-1.8	82	-0.15	5.3		
G-dCTP(1000)	**-0.84**	**220**	**-0.12**	**12**	**-0.063**	**0.67**

Y766A (contd)						
Reaction (μM dNTP)	**A_1(V)**	**k_1(s^{-1})**	**A_2(V)**	**k_2(s^{-1})**	**A_3(V)**	**k_3(s^{-1})**
T-dATP(1000) Fig. 4	**-0.24**	**120**				
T-dATP(1000, expt 2)	**-0.27**	**110**				
T-dATP(1000, expt 3)	**-0.26**	**95**				
E710A						
Reaction (μM dNTP)	**A_1(V)**	**k_1(s^{-1})**	**A_2(V)**	**k_2(s^{-1})**	**A_3(V)**	**k_3(s^{-1})**
G-dCTP(1000) Fig. 4	**-1.2**	**59**				
G-dCTP(1000, expt 2)	**-1.1**	**57**				
T-dATP(1000) Fig. 4	**-0.39**	**59**	**0.015**	**0.31**		
T-dATP(1000, expt 2)	**-0.23**	**43**	**0.013**	**0.27**		
T-dATP(1000, expt 2)	**-0.36**	**58**	**0.015**	**0.98**		
E710Q						
Reaction (μM dNTP)	**A_1(V)**	**k_1(s^{-1})**	**A_2(V)**	**k_2(s^{-1})**	**A_3(V)**	**k_3(s^{-1})**
C-dGTP(1000) Fig. S6A	**-0.40**	**40**				
C-dGTP(1000, expt 2)	**-0.39**	**47**				

[a] Stopped flow traces were fitted to single, double or triple exponential equations, as necessary to achieve satisfactory fits, and the amplitude (A) and rate constant (k) parameters are reported. The entries in bold contributed to the data reported in Table 3. Where more than one set of parameters are reported for a given substrate concentration, the first corresponds to the trace in the listed figure panel; entries designated "expt 2" etc are duplicate measurements that generated the averages reported in Table 3.

[b] Unlike the other Pol I(KF) mutants examined, the E710A mutant gave a low amplitude fluorescence decrease similar to what is usually observed with mispaired dNTPs. Two fit curves are shown as examples, but traces of this type are typically difficult to fit satisfactorily.

Table S2: Curve-fitting parameters derived from the FRET-based stopped-flow experiments reported in Tables 4 and 5.[a]

Protein	Reaction	A_1(V)	k_1(s^{-1})	A_2(V)	k_2(s^{-1})
Fingers-closing (Table 4)					
WT	A-dTTP (100 μM), Fig. 8A	0.54	100	0.17	22
WT	T-dATP (100 μM), Fig. 8B	0.28	430	0.048	8.6
WT	C-dGTP (50 μM), Fig. S7B	0.65	1100	0.067	79
WT	G-dCTP (50 μM), Fig. S7A	0.34	490	0.090	65
WT	G-dCTP (1 μM), Fig. 9D	0.40	19		
WT	G-dCTP (10 μM), Fig. 9D	0.69	89		
WT	G-dCTP (100 μM), Fig. 9D	0.31	250		
Y766A	G-dCTP (1 μM), Fig. 9C	0.075	15		
Y766A	G-dCTP (10 μM), Fig. 9C	0.17	65		
Y766A	G-dCTP (100 μM), Fig. 9C	0.15	170		
E710A	T-dATP (1 mM), Fig. 10B	0.11	77		
E710A	G-dCTP (1 mM), Fig. 10C	0.13	79	0.34	0.34
Y766F	A-dTTP (10 μM)	0.077	5.9		
(Fig. S8)	A-dTTP (20 μM)	0.16	250	0.038	3.9
	A-dTTP (50 μM)	0.20	85	0.076	3.5
	A-dTTP (100 μM)	0.38	68	0.10	6.4
	A-dTTP (200 μM)	0.43	65	0.13	11
Dissociation from template A (Fig. 11 and Table 5)					
Protein	**Nucleotide present in trap**	**A_1(V)**	**k_1(s^{-1})**	**A_2(V)**	**k_2(s^{-1})**
WT	None (binary complex)	-0.43	3.1		
	dTTP (2 mM)[b]	0.128	240	-0.50	0.75
	dATP (2 mM)	-0.36	20		
	dCTP (2 mM)	-0.37	14		
	dGTP (2 mM)	-0.35	28		
	rUTP (2 mM)	-0.40	20		
Y766F	None (binary complex)	-0.47	4.7		
	dTTP (2 mM)[b]	0.11	73	-0.50	0.72
	dATP (2 mM)				
	dCTP (2 mM)	-0.36	13		
	dGTP (2 mM)	-0.32	26		
	rUTP (2 mM)	-0.42	18		
Y766A	None (binary complex)	-0.17	22		
	dTTP (2 mM)	-0.12	19		
	dATP (2 mM)	-0.089	32		
	dCTP (2 mM)	-0.12	55		
	dGTP (2 mM)	-0.14	74		
	rUTP (2 mM)	-0.088	40		

Dissociation from template A (contd)					
Protein	**Nucleotide present in trap**	**A_1(V)**	**k_1(s^{-1})**	**A_2(V)**	**k_2(s^{-1})**
E710A	None (binary complex)	-0.19	6.8	-0.23	2.5
	dTTP (2 mM)	-0.28	22	-0.047	5.1
	dATP (2 mM)	-0.33	25	-0.031	3.3
	dCTP (2 mM)	-0.31	22	-0.064	6.3
	dGTP (2 mM)	-0.19	38	-0.17	9.4
	rUTP (2 mM)	-0.32	25	-0.048	4.4

[a] Stopped flow traces were fitted to single or double exponential equations, as necessary to achieve satisfactory fits, and the amplitude (A) and rate constant (k) parameters are reported. The averages in Tables 4 and 5 were derived from these data combined with data from additional duplicate experiments.

[b] In the presence of dTTP, the initial rapid fluorescence decrease corresponds to fingers-closing, and is followed by the fluorescence increase that results from DNA dissociation.